

Strange and Unconventional Isotope Effects in Ozone Formation

Yi Qin Gao and R. A. Marcus*

The puzzling mass-independent isotopic enrichment in ozone formation contrasts markedly with the more recently observed large unconventional mass-dependent ratios of the individual ozone formation rate constants in certain systems. An RRKM (Rice, Ramsperger, Kassel, Marcus)-based theory is used to treat both effects. Restrictions of symmetry on how energy is shared among the rotational/vibrational states of the ozone isotopomer, together with an analysis of the competition between the transition states of its two exit channels, permit the calculation of isotope effects consistent with a wide array of experimental results.

A puzzling “mass-independent” isotope effect, reported in 1973 for $^{16}\text{O}/^{17}\text{O}/^{18}\text{O}$ ratios in meteorites initially was attributed to nucleosynthetic processes (1). The validity of that description is still uncertain. In 1981, the enrichment of ^{18}O in ozone in the upper atmosphere was observed (2–6), and in 1983, the mass-independent effect was found for ozone formation in the laboratory (7–15) and then in the upper atmosphere (16–18). Laboratory studies of the formation of ozone from the recombination of oxygen atoms and oxygen molecules have shown that there is an approximately equal enrichment of ^{17}O and ^{18}O over ^{16}O , instead of the enrichment ratio being the standard, mass-dependent value described in the literature (19, 20) of close to one-half that found in other reactions [see also (21–24)]. A “mass-independent” effect is also seen in heavily enriched mixtures (25–29). More recently, and paradoxically, large unconventional mass-dependent isotopic effects were observed under special experimental conditions (“unscrambled” conditions, i.e., little complication from isotopic exchange) (30–33). The theoretical treatment given in this paper is designed to treat mass-independent and mass-dependent processes, as well as others (5, 12–15, 34–41), and to show that there are two distinctly different effects in the theory, one dominant in the scrambled and the other dominant in the unscrambled experiments.

It was once thought that the explanation of the mass-independent effect might have a simple symmetry origin: In the formation of ozone with trace ^{17}O and ^{18}O , these isotopes have in common that they alone can form an asymmetric isotopomer, e.g., $^{17}\text{O} + ^{16}\text{O}^{16}\text{O} \rightarrow ^{17}\text{O}^{16}\text{O}^{16}\text{O}$. Statistically, $^{16}\text{O}^{16}\text{O}^{16}\text{O}$ possesses,

because of the symmetry of the symmetric ozone, one-half the number of quantum states that $^{17}\text{O}^{16}\text{O}^{16}\text{O}$ and $^{18}\text{O}^{16}\text{O}^{16}\text{O}$ do. However, it was subsequently recognized that this simple statistical factor of 1/2 is automatically incorporated into the definition of the enrichment [see also (24)], and so a different explanation was needed—even if it might involve symmetry in a subtler role (42, 43).

Here, we present a theory which draws upon the statistical [RRKM (Rice, Ramsperger, Kassel, Marcus)] theory of unimolecular dissociation/bimolecular recombination reactions (44, 45) in its variational form (46–49). It initially involves the formation of vibrationally excited ozone isotopomers from the recombination of O and O_2 .

RRKM theory. In RRKM theory (50) for a bimolecular recombination $\text{X} + \text{YZ} \rightarrow \text{XYZ}^*$ (asterisk denotes a vibrationally excited molecule), the vibrational-rotational energy of XYZ^* is assumed to be statistically distributed among its vibrational-rotational modes, consistent with the given total energy E of those modes (that is, a microcanonical distribution) and total angular momentum J . The molecule can redissociate, $\text{XYZ}^* \rightarrow \text{XY} + \text{Z}$ or $\text{X} + \text{YZ}$, or lose or gain in its excess energy by collisions, the losing being the more prominent, and eventually form a stabilized XYZ molecule. In the present instance of ozone formation, X, Y, and Z may be the same isotope or any combination of different isotopes ^{16}O , ^{17}O , ^{18}O .

Because of the statistical assumption and the use of transition state theory (50), the unimolecular dissociation rate constant k_{EJ} for a vibrationally excited molecule of vibrational-rotational energy E and total angular momentum J is (44–48)

$$k_{EJ} = N_{EJ}^{\dagger} / h \rho_{EJ} \quad (1)$$

where N_{EJ}^{\dagger} is the number of quantum states accessible to the “transition state” for the dissociation for the given E and J and ρ_{EJ} is

the density (number per unit energy) of quantum states of the vibrationally excited molecule. The bimolecular rate constant to form this hot molecule is given by a related expression, e.g., (42, 43, 49), because of “microscopic reversibility.”

Nonstatistical aspects. As a modification of RRKM theory, it is argued that the effective ρ_{EJ} in Eq. 1 might be less than the statistical value, and more so for the symmetric isotopomers XYX^* than for XYZ^* . This ρ_{EJ} should be only the density of the quantum states of the triatomic molecule that are sufficiently dynamically coupled to the two “exit channels” that they can lead to the dissociation of the molecule in the typical lifetime of the latter: After the formation of the vibrationally excited molecule, the subsequent redistribution of the energy among its vibrational-rotational modes at the given E and J proceeds at some finite rate and may be incomplete during the typical lifetime of the molecule (the non-RRKM effect). The ρ_{EJ} in Eq. 1 should then refer only to the quantum states which have been equilibrated intramolecularly.

Examples are known from various experiments, e.g., (51–53), which illustrate the time needed for this internal equilibration of isolated molecules. Because there are fewer dynamical coupling terms (e.g., anharmonic vibration-vibration and Coriolis vibration-rotation) in the symmetric XYX than in the asymmetric XYZ , some terms being forbidden by the symmetry, it was suggested (42, 54) that this nonstatistical (non-RRKM) effect for ρ_{EJ} is expected to be greater for XYX than for XYZ . This idea remains to be tested by direct real-time experiments or by very detailed accurate quantum dynamical calculations yet to be made.

The situation just described is depicted schematically in the cartoon in Fig. 1: during the typical lifetime of the dissociating ozone, the shaded regions indicate the ozone quantum states sufficiently strongly coupled dynamically to the two exit channels so as to contribute to ρ_{EJ} during that lifetime. The shaded region for the asymmetric molecule is drawn as a greater fraction of the total region than is that for the symmetric molecule for the dynamics-based reason given above. The ratio of the fraction of shaded to total region for the asymmetric molecule to the same fraction for the symmetric molecule is denoted by η , a symbol introduced previously for this purpose (42, 54).

New features in present treatment. In a recent article (43), which applied these ideas in (42), the simplest possible transition state for the reaction $\text{X} + \text{YZ} \rightarrow \text{XYZ}^*$ was assumed for convenience, namely, a transition state XYZ^{\ddagger} , frequently called “loose,” in which the YZ rotates freely. The transition state for a barrierless recombination reaction is typically loose when the energy of the recombining particles is low

Noyes Laboratory of Chemical Physics, Mail Code 127-72, California Institute of Technology, Pasadena, CA 91125, USA.

*To whom correspondence should be addressed. E-mail: ram@caltech.edu

enough, e.g., (43, 55–58). However, more generally, it is expected that the rotation of YZ is somewhat hindered in the transition state XYZ^\ddagger , particularly with increasing total vibrational-rotational energy E of the ozone (43, 49, 55–58). If, as at low energies, the $O_2 \dots O$ distance in the O_3^\ddagger transition state is large, the O_2 indeed can rotate more or less freely. Although this simple assumption of free rotation of the O_2 in O_3^\ddagger was very useful in (43), we avoided it here in order to generalize this previous work and so include in the treatment a much wider range of experimental temperatures and pressures. The two approaches are compared in (49).

A second major difference between the treatment in this paper and that in (42, 43) is the elimination of a “strong collision” assumption: it was assumed in (43) that every collision of the XYZ^* with a molecule M in the surrounding gas deactivates (and so stabilizes) an XYZ^* . In the case of “weak” collisions, on the other hand, the average energy lost by XYZ^* in “downward” collisions (ΔE) and the energy gained in “upward” collisions can be relatively small. Some limited information on collisional energy transfer with vibrationally hot molecules such as XYZ^* is available in the literature from experiments and from classical trajectory calculations (59–62). A “master equation” (47–49) is now used to treat these weak collisions. The limitation imposed by weak collisions is profound: only XYZ^* molecules with low energies (excess above threshold) can be deactivated at low pressures, when collisions are few, thereby affecting various properties, as listed in Table 1.

To determine the nature of the transition state (e.g., loose, “tight,” hindered), variational RRKM theory can be used, but some potential-energy surface for the ozone formation is need-

ed. At present, the ab initio surface in the literature (63) is inadequate. For example, there should be no energy barrier in the entrance channel from $X + YZ$ (64). The use of an empirically modified surface (65) that eliminates this barrier led to results that disagreed (49) with the known isotopic exchange rate data. In the interim, we have adopted (49) an approximate model that is consistent with those data. The potential-energy surface and the calculation of the number of states N_{EJ} along the reaction coordinate in a given exit channel serve to determine variationally (50) the transition state (TS) for that channel, whose N_{EJ} is then denoted by N_{EJ}^\ddagger and appears in Eq. 1. The choice of transition state affects mostly the pressure effects and the temperature effects at higher pressures, and the isotopic exchange reactions, but it also has some influence on the other quantities listed in Table 1.

Application to ozone formation. We consider a reaction scheme involving recombination, deactivation, activation, and redissociation, given by $X + YZ \rightarrow XYZ^*$, $XYZ^* \rightarrow X + YZ$, $XYZ^* \rightarrow XY + Z$, and, further, a series of collisional activation/deactivation steps that can lead eventually to a full deactivation, $XYZ^* + M \rightarrow XYZ + M$. The second and third steps represent the two dissociative exit channels from XYZ^* , a and b , and are equivalent when $Z = X$. As a convention in these studies, a was chosen (42) to be the exit channel with the lower zero-point energy of the diatomic molecule. The bimolecular rate constant of the above reaction, $X + YZ \rightarrow XYZ$, is denoted below by k_{bi}^a or k_{bi}^b , according to whether YZ or XY has the lower zero-point energy.

An expression can be obtained for the net bimolecular reaction rate constant k_{bi} for the recombination: To implement the collisional deactivation/activation scheme, we employed (49) for simplicity a “stepladder” model (48), in which the XYZ^* gains or loses its energy in collisions in discrete amounts (“steps”), ΔE . In the interests of brevity, we use as an illustration here an expression for k_{bi} that is a special case of our more general results: We consider the special case where there is only one step of the ladder that is reactive but where there are any number of steps below the dissociation threshold of XYZ^* (66). We then have (66)

$$k_{bi}^a = \sum_J \int_{\Delta E} \frac{k_a k_{diff}}{k_a + k_b + k_{diff}} g_{eq} dE \quad (2)$$

where $k_{a,b} \equiv k_{a,b}(EJ)$ is the dissociation rate constant given by Eq. 1. The k_{diff} denotes the rate constant for the stepwise collisional deactivation of XYZ^* (a stepwise “diffusion” process in energy space), and g_{eq} is the equilibrium distribution function of the (EJ) states of XYZ^* . The integration over E spans an interval equal to the step size ΔE , and the summation (or integration) is over all J . At low pressures, the k_{diff} in the denominator can be neglected, and in that case the factor $k_d/(k_a + k_b)$ in the integrand plays a prominent role for the individual rate constants. It equals $N_{EJ}^\ddagger/(N_{EJ}^\ddagger + N_{EJ}^\ddagger)$ and was termed the partitioning factor Y_a in (42, 43), because it “partitions” the dissociation fate of XYZ^* into the two dissociation channels. The “strong collision” model used in (42, 43) can be retrieved from Eq. 2 by letting ΔE become very large. In that case, it can also be shown that k_{diff} equals ω , the collision frequency appearing in (42, 43).

Table 1. Comparison of experiment and theory. All quantities in units of $\text{cm}^3 \text{ molecule}^{-1} \text{ s}^{-1}$ are to be multiplied by 10^{-12} . In the last column, the quantities in parentheses are less important. The quantities are defined in the text.

Experiments	Calculated results	Sensitivity
Ratios of rate constants, Figs. 2 and 3 (28, 30–33)	Figs. 2 and 3	$\Delta E, Y, \eta$
Enrichments ^{17}O (11.3%), ^{18}O (13.0%) at 300 K (7–15)	12.0 and 12.2%, respectively	$\eta, (\Delta E)$
Heavily enriched systems, Fig. 4 (25–29)	Fig. 4	$\eta, (\Delta E)$
Low pressure $^{16}\text{O} + ^{32}\text{O}_2 + M \rightarrow ^{48}\text{O}_3 + M$, $k_{bi} = 5 \times 10^{-34} \text{ cm}^6 \text{ molecule}^{-2} \text{ s}^{-1}$ (41)	$9 \times 10^{-34} \text{ cm}^6 \text{ molecule}^{-2} \text{ s}^{-1}$	ΔE
$k_{bi} \propto T^{-n}$, $n = 2.6$ (130 to 300 K) (41)	$n = 2.2$	ΔE
$k_{ex} \text{ } ^{16}\text{O} + ^{18}\text{O}^{18}\text{O} \rightarrow ^{16}\text{O}^{18}\text{O} + ^{18}\text{O}$, $2.9 \pm 0.8 \text{ cm}^3 \text{ molecule}^{-1} \text{ s}^{-1}$ (300 K), $5.6 \text{ cm}^3 \text{ molecule}^{-1} \text{ s}^{-1}$ (130 K), $k_{ex} \propto T^{-m}$, $m = 0.88 \pm 0.26$ (38, 40)	Fitted to data: $2.7 \text{ cm}^3 \text{ molecule}^{-1} \text{ s}^{-1}$ (300 K), $4.3 \text{ cm}^3 \text{ molecule}^{-1} \text{ s}^{-1}$ (130 K), $m = 0.53$	TS
High-pressure k_{bi} $^{16}\text{O} + ^{32}\text{O}_2 \rightarrow ^{48}\text{O}_2$, $18 \text{ cm}^3 \text{ molecule}^{-1} \text{ s}^{-1}$ (130 K), $>4 \text{ cm}^3 \text{ molecule}^{-1} \text{ s}^{-1}$ (300 K) (limiting value not reached) (41)	$10.4 \text{ cm}^3 \text{ molecule}^{-1} \text{ s}^{-1}$ (130 K), $6.5 \text{ cm}^3 \text{ molecule}^{-1} \text{ s}^{-1}$ (300 K)	TS, ΔE (at high T)
Pressure effects on enrichments (14, 15)	Broad agreement (49)	$\eta, (\Delta E)$
Pressure effects on rate constant ratios (33)	Broad agreement (49)	$\Delta E, Y, \eta$
Temperature effect on rate constant ratios	Approximate prediction from temperature effect on enrichments δ^Q	$\Delta E, Y, \eta$
Temperature effect on enrichment (15)	Used to calculate previous row	$\eta, (\Delta E)$

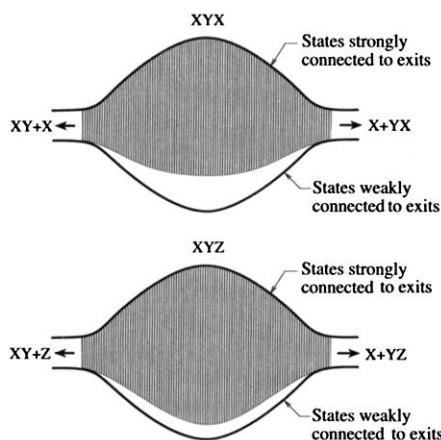


Fig. 1. Schematic picture for XYX and for XYZ of differences in ratios of rotational-vibrational states of ozone strongly coupled (shaded region) to the two dissociation exit channels of ozone and those that weakly coupled (unshaded region) to the exit channels. This difference in ratios has an origin in symmetry, as noted in the text and discussed in (42). In one limit, the unshaded region is absent for XYZ.

Enrichments. The enrichment δ of ^{17}O and that of ^{18}O over ^{16}O in the formation of ozone, denoting the ^{17}O or ^{18}O by Q, is defined by (67, 68)

$$\delta^Q = \frac{Q/O \text{ in ozone}}{Q/O \text{ in oxygen}} - 1 \quad (3)$$

Expressions for each δ^Q were given in (42) in terms of the individual rate constants and certain equilibrium constants.

When the study focuses, instead, on systems heavily enriched in ^{17}O and/or ^{18}O , the definition used for the enrichment for an ozone molecule of mass M relative to $^{48}\text{O}_3$ is E^M (25, 42)

$$E^M = \left[\frac{\binom{M}{^{48}\text{O}_3}}{\binom{M}{^{48}\text{O}_3}_{\text{meas}}} \bigg/ \frac{\binom{M}{^{48}\text{O}_3}}{\binom{M}{^{48}\text{O}_3}_{\text{calc}}} \right] - 1 \quad (4)$$

The denominator in Eq. 4 is calculated statistically from the isotopic composition of the O_2 (42). The E^M can be shown to reduce to the δ^Q upon reducing the mole fractions of ^{17}O and ^{18}O to trace amounts (49).

Individual rate constants and ratios. The ratios of rate constants calculated for the specific isotopomeric recombination reactions, $X + YZ \rightarrow XYZ$, are used to compare with the experimental data on them and also to calculate the enrichments δ^Q and E^M (69) and compare with the data on the latter. The expression (42, 43) for the exchange rate constants $X + YY \rightarrow XY + Y$ at low pressures, where the measurements of the isotopic exchange rates are made, was also readily obtained (42, 43): In the solution of the master equation, in the low-pressure limit we note that the large majority of XYZ^* molecules will redissociate. When dissociation occurs via the other exit channel, an isotopic exchange has occurred. A simple expression for the isotopic exchange rate constant was then obtained, which is independent of the details of the collision process (42).

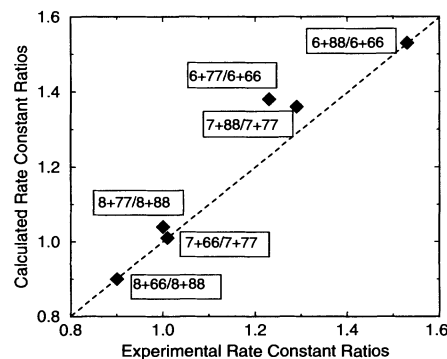


Fig. 2. Comparison of calculated and experimental (28) relative atom + diatomic rate constant ratios, k_{X+YZ}/k_{X+XX} , at 300 K with $\eta = 1.18$. A typical symbol in a box, such as 8+77/8+88, refers to the ratio of rate constants for $^{18}\text{O} + ^{17}\text{O}^{17}\text{O} \rightarrow ^{18}\text{O}^{17}\text{O}^{17}\text{O}$ to $^{18}\text{O} + ^{18}\text{O}^{18}\text{O} \rightarrow ^{18}\text{O}^{18}\text{O}^{18}\text{O}$. The (uncertain) concentration ^{18}O cancels when the ratios of such rate constants are obtained from mass spectrometric measurements.

The individual recombination rate constants at low pressures were obtained using a more elaborate version of Eq. 2, one which involves the detailed solution of the master equation for the collisional deactivation/activation and reaction steps, for many "steps" in the stepladder (49). A $\Delta E \sim 210 \text{ cm}^{-1}$ was used for the deactivating collisions (49). The two quantities, ΔE and $\eta (= 1.18)$, were chosen to fit the two experimentally measured rate constant ratios at 300 K, $^{16}\text{O} + ^{18}\text{O}^{18}\text{O}/^{16}\text{O} + ^{16}\text{O}^{16}\text{O}$ and $^{18}\text{O} + ^{16}\text{O}^{16}\text{O}/^{18}\text{O} + ^{18}\text{O}^{18}\text{O}$ (70).

We note in passing that in Eq. 2, k_{diff} and the ρ_{EJ} in the k 's occur as a product, since the k_{EJ} (here, k_a and k_b) in Eq. 1 is proportional to $1/\rho_{EJ}$ and the g_{eq} is proportional to ρ_{EJ} . Thereby, all results for the present data would be unchanged if the η -effect were ascribed instead to a k_{diff} as examined in (49).

Results. The various experimental results (Table 1 and Figs. 2 through 4) are compared with the calculations. The results in Figs. 2 and 3 for the "unscrambled systems" show a strong and unconventional mass-dependence. Their correlation with ratios of masses given in figure 3 of (43) contrasts with the usual isotopic mass-dependence described for other reactions in a pioneering paper (71). The results in Fig. 4 for E^M and those for δ^Q for trace systems show the "mass-independence". Although the enrichments of all isotopomers $XY + YXY$ in Fig. 4 are not exactly equal, i.e., strictly mass-independent, they are seen to vary far less widely than the ratios of k_{bi} values do in Figs. 2 and 3. We have also indicated in Table 1 the relative importance of the various properties Y , η , ΔE , and TS (transition state) in each type of measurement.

Discussion. In the formation of ozone, the insertion reaction of O into O_2 is assumed to be negligible, in agreement with current data (32). Before proceeding to discuss the present results, we first comment on the heart of the explanation (42, 43) for the paradox described earlier: Under

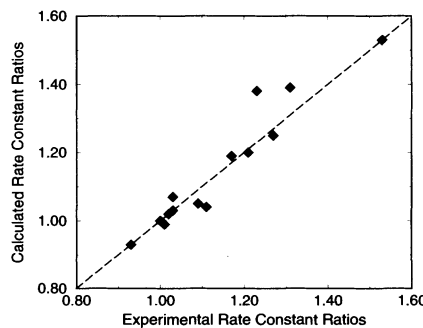


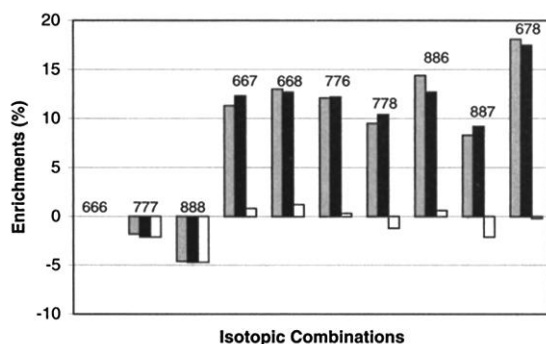
Fig. 3. Comparison of calculated and experimental (28) relative atom + diatomic rate constant ratios, k_{X+YZ}/k_{6+66} , at 300 K with $\eta = 1.18$. Some of the experimental rate constants are "derived quantities" (28). The 6+66 denotes the recombination reaction $^{16}\text{O} + ^{16}\text{O}^{16}\text{O} \rightarrow ^{16}\text{O}^{16}\text{O}^{16}\text{O}$.

unscrambled conditions, the vibrationally hot molecule XYZ^* is formed only from one entrance channel, the channel depending on the initial choice of reactants. Small differences in zero-point energies of these two entrance or exit channels lead to major effects on k_{bi}^a and k_{bi}^b . The unexpected effect of small differences in zero-point energies on the individual rate constants and rate constant ratios occurs by affecting the partitioning factors Y_a and Y_b . At the lowest energies, $Y_a = 1$ and $Y_b = 0$, whereas once the zero-point energy of b has been exceeded, the number of states $N_{EJ}^{b\dagger}$ grows approximately as the square of its excess energy above this zero-point energy (49), but meanwhile $N_{EJ}^{a\dagger}$ has been growing roughly as the square of its excess over its zero-point energy. The result is a large difference (49) in Y_a and Y_b for most of the energy region of interest at low pressures (energies less than the step size), and so a k_{bi}^a can be quite large. For k_{bi}^b , in contrast, there is no low-energy region where $Y_b = 1$. Instead, Y_b typically begins at $Y_b \approx 0$. In (43) it was shown that the individual recombination rate constants k_{bi} correlated well with a property that depended only on certain differences in masses, namely, zero-point energies, moments of inertia, or reduced masses, all of three of which were shown to be simply related to each other [compare figure 3 in (43) and the remarks in its legend and in section VI there]. Indeed, in the theory all three properties contribute to Y_a and Y_b (43).

Under isotopically "scrambled" conditions—i.e., conditions where extensive isotopic exchange affects the observations—both entrance channels leading to XYZ^* are accessed and it was shown mathematically that the partitioning factors Y_a and Y_b have disappeared (42). The essence of the underlying physical basis is surprisingly simple: entrance via the a channel yields a Y_a factor at low pressures, whereas entrance via the b channel yields Y_b . The sum $Y_a + Y_b$ is unity and so for the enrichments, the partitioning factors and their dramatic nonconventional isotope effect have vanished, because of this access to XYZ^* from both entrance channels. The nonstatistical effect mentioned earlier is the only influence now left and yields the "mass-independent" effect (42, 43), which is exhibited in Fig. 4 and in Table 1. The disappearance of the partitioning factors in the enrichment experiments yields the dramatic effect in Fig. 4, seen in the marked contrast between the $\eta = 1$ and the $\eta = 1.18$ results.

As the above discussions of the theory illustrate, there are two types of isotope effects in the theory for the phenomena: There is the partitioning effect between the two competing transition states, which affects strongly the ratios of rate constants measured in "unscrambled" experiments, as in Figs. 2 and 3. There is also the non-RRKM effect in the ozone molecule itself, namely, a deviation from the statistical (RRKM, microcanonical) density of states ρ_{EJ} of the ozone isotopomer itself, and which

Fig. 4. Experimental (28) (gray bars) and calculated isotopic enrichments for scrambled systems heavily enriched in heavy isotopes at 300 K, with $\eta = 1.18$ (black bars) and $\eta = 1.0$ (white bars), respectively. A typical symbol, such as 668, denotes an ozone with the isotopic composition $^{16}\text{O}^{16}\text{O}^{18}\text{O}$ and consists of the asymmetric ($^{16}\text{O}^{16}\text{O}^{18}\text{O}$) and symmetric ($^{16}\text{O}^{18}\text{O}^{16}\text{O}$) isotopomers.



differs for vibrationally excited symmetric (XYX) as compared with asymmetric (XYZ) ozone molecules. It is the principal factor affecting the enrichments. Thus, the two types of isotope effects, which are seen to have distinctly different theoretical origins, are also revealed separately by the two types of experiments, scrambled and unscrambled.

The comparison of many experiments and theory is summarized in Table 1. We first note that in the large body of experimental data listed there, some data are sensitive to the weak collision aspect, ΔE , but relatively insensitive to the nature of the transition state, whereas others are sensitive to the partitioning factors Y . Still others are sensitive to the nature of the potential-energy surface and the transition state, and are denoted in Table 1 by TS. We have indicated in Table 1 which measurements are sensitive most to each of the quantities ΔE , Y , η , and TS. For example, all of the data in Figs. 2 through 4, the low-pressure k_{bi} for $^{16}\text{O} + ^{32}\text{O}_2 \rightarrow ^{48}\text{O}_3$ and its temperature exponent n , are dependent on ΔE , the mean downward energy transferred from the XYZ^* per collision, but are relatively insensitive to TS, in particular to the short-range effects of the potential-energy surface (49). The temperature effect on the individual rate constants is influenced by ΔE : the smaller the value of ΔE , the larger the negative exponent n in Table 1, since a smaller ΔE implies that a smaller proportion of the reacting molecules at the higher temperatures can contribute to the recombination rate at low pressures.

We have not shown the pressure effects on the enrichments and individual rate constant ratios but note that we have found the calculated results to be in reasonable agreement with the experiments (49, 72). The temperature effect on enrichment (15) remains to be explored theoretically, but one factor may be a decrease in η with decreasing temperature, because of a longer lifetime of O_3^* at low temperatures and so more time for redistribution. Dynamical information on η and ΔE can be inferred from temperature effects, within the assumptions of the present theory. Given an experimentally measured enrichment δ^Q for $Q = 17$, or 18 at other temperatures, predictions can be made of the various k_{bi}^a and k_{bi}^b values at those temperatures (49), and

an example is given in (49).

The present results provide a rationale for an ad hoc assumption used in (43), though not here. In (43), a "loose transition state," which is appropriate for low energies, was used, together with strong collisions, to treat the experimental data in Figs. 2 through 4. The ad hoc assumption was that the ratios of these rate constants would approximate the ratios at room temperature, even though the latter have a hindered transition state. The existence of the present ΔE tends to limit the actual low-pressure studies to low energies. Thus, ozone molecules formed with an energy excess over the threshold greater than ΔE are not deactivated in a single collision regime, which is the regime occurring at low pressures, so providing a rationale for the use in (43) of low-energy k_{bi} values.

The key isotope effects in the present paper, η and Y , are in a sense symmetry-driven: the deviation of the Y values from 1/2 occurs for the asymmetric isotopomers, and the Y values are responsible for the large differences in individual rate constants and their ratios. The origin of η is also a consequence of symmetry.

Isotopic effects are widely studied for other reactions in the upper atmosphere, though not yet in the detail accorded to the ozone formation. For gas-phase reactions where symmetric intermediates can occur, the η would again enter, whereas for intermediates that are structurally asymmetric, the isotopic effect on η would disappear. However, some of the isotopic effect on Y can survive, leading to unconventional isotope effects. Thoroughly detailed studies of the type available for ozone would be highly desirable for these other reactions and would assist in the detailed understanding of them. Unconventional isotope effects have been invoked in discussions of stratospheric/atmospheric mixing, oxidative processes in the upper atmosphere, and ancient and Martian atmospheres (73–76).

References and Notes

- R. N. Clayton *et al.*, *Science* **182**, 485 (1973).
- K. Mauersberger, *Geophys. Res. Lett.* **8**, 935 (1981).
- M. M. Abbas *et al.*, *J. Geophys. Res.* **92**, 13231 (1987).
- B. Carli, J. H. Park, *J. Geophys. Res.* **93**, 3851 (1988).
- F. W. Irion *et al.*, *Geophys. Res. Lett.* **23**, 2377 (1996).

- D. Krankowsky *et al.*, *Geophys. Res. Lett.* **27**, 2593 (2000).
- J. E. Heidenreich III, M. H. Thiemens, *J. Chem. Phys.* **78**, 892 (1983).
- M. H. Thiemens, J. E. Heidenreich III, *Science* **219**, 1073 (1983).
- J. Yang, S. Epstein, *Geochim. Cosmochim. Acta* **51**, 2011 (1987).
- M. H. Thiemens, T. Jackson, *Geophys. Res. Lett.* **14**, 624 (1987).
- J. E. Heidenreich III, M. H. Thiemens, *J. Chem. Phys.* **84**, 2129 (1986).
- M. H. Thiemens, T. Jackson, *Geophys. Res. Lett.* **15**, 639 (1988).
- S. K. Bains-Sahota, M. H. Thiemens, *J. Phys. Chem.* **91**, 4370 (1987).
- M. H. Thiemens, T. Jackson, *Geophys. Res. Lett.* **17**, 717 (1990).
- J. Morton *et al.*, *J. Geophys. Res.* **95**, 901 (1990).
- K. Mauersberger, *Geophys. Res. Lett.* **14**, 80 (1987).
- B. Schueler *et al.*, *Geophys. Res. Lett.* **17**, 1295 (1990).
- D. Krankowsky *et al.*, *Geophys. Res. Lett.* **22**, 1713 (1995).
- An excellent review of the conventional (mass-dependent) effect in chemistry, as well as of the history of the mass-independent effect and of previous attempts to explain it, is given in (20). This also includes an updated review of a correlation-symmetry view of the mass-independent effect in (21). An early review and theoretical examination of the mass-independent effect is given in (23).
- R. E. Weston Jr., *Chem. Rev.* **99**, 2115 (1999).
- G. I. Gellene, *Science* **274**, 1344 (1996), and references cited therein.
- J. A. Kaye, D. F. Strobel, *J. Geophys. Res.* **88**, 8447 (1983).
- J. A. Kaye, *J. Geophys. Res.* **91**, 7865 (1986).
- S. M. Anderson, J. A. Kaye, *Geophys. Res. Lett.* **24**, 91 (1987).
- J. Morton *et al.*, *Chem. Phys. Lett.* **154**, 143 (1989).
- K. Mauersberger *et al.*, *Geophys. Res. Lett.* **20**, 1031 (1993).
- D. Krankowsky, K. Mauersberger, *Science* **274**, 1324 (1996).
- K. Mauersberger *et al.*, *Science* **283**, 370 (1999).
- S. Wolf *et al.*, *J. Chem. Phys.* **113**, 2684 (2000).
- S. M. Anderson *et al.*, *J. Chem. Phys.* **107**, 5385 (1998).
- J. Günther *et al.*, *Chem. Phys. Lett.* **306**, 209 (1999).
- C. Janssen *et al.*, *J. Chem. Phys.* **111**, 7179 (1999).
- J. Günther *et al.*, *Chem. Phys. Lett.* **324**, 31 (2000).
- J. C. Johnston, M. H. Thiemens, *J. Geophys. Res.* **102**, 25395 (1997).
- J. Sehested *et al.*, *J. Geophys. Res.* **100**, 20979 (1995).
- L. K. Christensen *et al.*, *J. Mol. Spectrosc.* **175**, 220 (1996).
- A. Meier, J. Notholt, *Geophys. Res. Lett.* **23**, 551 (1996).
- M. R. Wiegell *et al.*, *Int. J. Chem. Kinet.* **29**, 745 (1997).
- J. Sehested *et al.*, *J. Geophys. Res.* **103**, 3545 (1998).
- S. M. Anderson *et al.*, *J. Chem. Phys.* **83**, 1648 (1985).
- H. Hippler *et al.*, *J. Chem. Phys.* **93**, 6560 (1990).
- B. C. Hathorn, R. A. Marcus, *J. Chem. Phys.* **111**, 4087 (1999).
- _____, *J. Chem. Phys.* **113**, 9497 (2000).
- R. A. Marcus, *J. Chem. Phys.* **20**, 359 (1952).
- _____, *J. Chem. Phys.* **43**, 2658 (1965); *J. Chem. Phys.* **52**, 1018 (1970).
- D. M. Wardlaw, R. A. Marcus, *Adv. Chem. Phys.* **70**, 231 (1988).
- R. G. Gilbert, S. C. Smith, *Theory of Unimolecular and Recombination Reactions* (Blackwell Scientific, Boston, 1990).
- K. A. Holbrook, M. J. Pilling, S. H. Robertson, *Unimolecular Reactions* (Wiley, New York, ed. 2, 1996).
- Y. Q. Gao, R. A. Marcus, in preparation.
- Transition state theory, a theory in the chemical literature for some 65 years, is still the standard theory of choice for treating chemical reaction rates at a given temperature. Its counterpart for molecules of a given energy E is RRKM theory (microcanonical transition state theory), which was developed some 15 years later (44). In its usual formulation, either theory assumes a

- quasi-equilibrium between the reactant or reactants and the "transition state," a critical set of configurations from which, once reached, there is no return to the original reactant or reactants but rather the system proceeds to form the product or products. Because of the quasi-equilibrium aspect, concepts such as "free energy of activation" and "statistical mechanical partition function" appear in the canonical (i.e., temperature-based) transition state theory, and concepts such as number of quantum states N_{EJ}^{\ddagger} in the transition state and density of states ρ_{EJ} of the unimolecularly dissociating or isomerizing molecule appear in its microcanonical counterpart, RRKM theory (Eq. 1). The transition state for the forward reaction is the same as that of the reverse reaction and it occurs at the maximum of a free energy barrier in canonical transition state theory, or at the minimum of an entropy barrier (minimum N_{EJ}^{\ddagger}) at the given energy E and J in RRKM theory. This maximum or minimum property confers on it the title "variational transition state theory" or "variational RRKM theory."
51. I. Oref, B. S. Rabinovitch, *Acc. Chem. Res.* **12**, 166 (1979), and references cited therein.
52. R. Weinkauff *et al.*, *J. Chem. Phys.* **98**, 8381 (1994); see also (77).
53. S. K. Kim *et al.*, *J. Phys. Chem.* **100**, 9202 (1996).
54. The shaded region for XYZ in Fig. 1 was assumed to be absent in (42). This assumption affects only absolute rates, but has no effect on the ratios of the rate constants, and so no effect on the present Figs. 2 through 4.
55. W. L. Hase, *J. Chem. Phys.* **64**, 2442 (1976).
56. M. Quack, J. Troe, *Ber. Bunsenges. Phys. Chem.* **81**, 329 (1977).
57. G. P. Smith, D. M. Golden, *Int. J. Chem. Kinet.* **10**, 489 (1978).
58. S. J. Klippenstein, R. A. Marcus, *J. Chem. Phys.* **91**, 2280 (1989).
59. For example, G. Lendvay, G. C. Schatz, in *Adv. Chem. Kinet. Dyn.* **2B**, 481 (1995), and references cited therein.
60. J. R. Barker, B. M. Toselli, *Int. Rev. Phys. Chem.* **12**, 305 (1993), and references cited therein.
61. R. G. Gilbert, *Aust. J. Chem.* **48**, 1787 (1995).
62. A. J. Stace, J. N. Murrell, *J. Chem. Phys.* **68**, 3028 (1978).
63. C. Leforestier *et al.*, *J. Chem. Phys.* **101**, 3806 (1994).
64. The need for a barrierless potential-energy surface is reflected in the negative temperature coefficient of the various recombination and isotopic exchange reactions, e.g., in (45) and in (38), and also in Table 1, and in the absolute values of the rate constants given there. Apart from an electronic degeneracy factor, they are near gas-kinetic. The expression in (63) gives, instead, an energy barrier.
65. A. Gross, G. D. Billing, *Chem. Phys.* **217**, 1 (1999).
66. R. A. Marcus, Y. Q. Gao, *J. Chem. Phys.* **114**, 9807 (2001).
67. H. Craig, *Geochim. Cosmochim. Acta* **12**, 133 (1957).
68. Y. Matsuhisa, J. R. Goldsmith, R. N. Clayton, *Geochim. Cosmochim. Acta* **42**, 173 (1978).
69. The E^M was expressed in (42) in terms of the individually calculated recombination rate constants. To obtain an expression for these enrichments E^M and δ° and still allow for the numerous isotopomers of each species, it was noted that certain ratios of statistical mechanical partition functions (not the partitioning factors Y) were equal to unity, within several thousandths (42). This approximation provided a considerable simplification of a large number of reaction equations involving the many permutations of X, Y, and Z and led to simple final expressions in (42) involving individual rate constants k_{bi} and certain equilibrium constants.
70. For the present calculations of the rate constants and of the enrichments E^M for the many isotopomers, only 26 of the 54 isotopomeric vibration frequencies were known, and the missing ones were needed in the calculations for densities of states ρ_{EJ} . A second-order perturbation formulation gave the unknown frequencies to an accuracy of about 1 cm^{-1} , quite sufficient for the present purpose (78). The long-range part of the interaction potential $-C_6/r^6$ was used in the calculation of the potential-energy surface, in addition to the short-range potential terms, C_6 being obtained from collision cross sections for $\text{O} + \text{O}_2$ (79). The anharmonicity effect on the density of states ρ_{EJ} was obtained from vibrational spectra of ozone molecules (80), by fitting those data to a theoretical expression containing the various anharmonicity constants (49). The various enrichments and rate constants were calculated using the relevant equations given in (42, 43) but now using the presently calculated values of the various k_{bi} values and of the various equilibrium constants appearing in those expressions.
71. J. Bigeleisen, M. G. Mayer, *J. Chem. Phys.* **15**, 261 (1947).
72. One effect on which we have not commented thus far is the role of collisions in stimulating vibrational energy redistribution within a molecule, a known process: In principle, some "active states" formed in the recombination, and so contributing to ρ_{EJ} , could be converted to the less active states by collision and so have their dissociative lifetime prolonged prior to the next collision. Unless the collision cross section for energy redistribution were extremely large, the calculated low-pressure results in Table 1 and Figs. 2 through 4 would be unaffected by these collisions at low pressures.
73. J. Farquhar *et al.*, *Science* **289**, 756 (2000).
74. H. Bao *et al.*, *Nature* **406**, 176 (2000).
75. M. H. Thiemens, *Science* **283**, 341 (1999).
76. ———, T. Jackson, E. C. Zipf, P. W. Erdman, C. van Egmond, *Science* **270**, 969 (1995).
77. R. Knochenmuss, *J. Phys. Chem.* **99**, 3381 (1995).
78. B. C. Hathorn, R. A. Marcus, *J. Phys. Chem. A* **105**, 5586 (2001).
79. B. Brunetti *et al.*, *J. Chem. Phys.* **74**, 6734 (1981), table I.
80. V. G. Tyuterev, S. Tashkun, P. Jensen, A. Barbe, T. Cours, *J. Mol. Spectrosc.* **198**, 57 (1999).
81. It is a pleasure to acknowledge the support of this research by the NSF and the helpful discussions with B. Hathorn in its early stages. We are very pleased to acknowledge helpful comments by K. Mauersberger, S. Anderson, M. Thiemens, R. Weston, and the reviewers.

21 December 2000; accepted 22 May 2001

Published online 31 May 2001;

10.1126/science.1058528

Include this information when citing this paper.

Ubiquitination of a New Form of α -Synuclein by Parkin from Human Brain: Implications for Parkinson's Disease

Hideki Shimura,^{1,2*} Michael G. Schlossmacher,^{1,2*†}
Nobutaka Hattori,⁴ Matthew P. Frosch,^{1,2,3}
Alexander Trockenbacher,⁵ Rainer Schneider,⁵
Yoshikuni Mizuno,⁴ Kenneth S. Kosik,^{1,2‡} Dennis J. Selkoe^{1,2‡}

Parkinson's disease (PD) is a common neurodegenerative disorder characterized by the progressive accumulation in selected neurons of protein inclusions containing α -synuclein and ubiquitin. Rare inherited forms of PD are caused by autosomal dominant mutations in α -synuclein or by autosomal recessive mutations in parkin, an E3 ubiquitin ligase. We hypothesized that these two gene products interact functionally, namely, that parkin ubiquitinates α -synuclein normally and that this process is altered in autosomal recessive PD. We have now identified a protein complex in normal human brain that includes parkin as the E3 ubiquitin ligase, UbcH7 as its associated E2 ubiquitin conjugating enzyme, and a new 22-kilodalton glycosylated form of α -synuclein (α Sp22) as its substrate. In contrast to normal parkin, mutant parkin associated with autosomal recessive PD failed to bind α Sp22. In an *in vitro* ubiquitination assay, α Sp22 was modified by normal but not mutant parkin into polyubiquitinated, high molecular weight species. Accordingly, α Sp22 accumulated in a non-ubiquitinated form in parkin-deficient PD brains. We conclude that α Sp22 is a substrate for parkin's ubiquitin ligase activity in normal human brain and that loss of parkin function causes pathological α Sp22 accumulation. These findings demonstrate a critical biochemical reaction between the two PD-linked gene products and suggest that this reaction underlies the accumulation of ubiquitinated α -synuclein in conventional PD.

Parkinson's disease is a highly prevalent neurodegenerative disorder that causes progressive motor dysfunction, variable cognitive impairment, and shortened life expectancy (1). The molecular pathogenesis of PD remains unclear, but genetic factors play a role in some cases. The genes encoding parkin (2), α -synuclein (α S) (3, 4), and ubiquitin

carboxyl-terminal hydrolase (UCH)-L1 (5) have each been linked to familial forms of PD. Missense mutations in α S or UCH-L1 cause rare, autosomal dominant forms of PD. In contrast, mutations of parkin are a relatively common cause of autosomal recessive PD (ARPD), which often has early onset (6, 7). As is the case in conventional ("idiopathic")